



You have downloaded a document from
RE-BUS
repository of the University of Silesia in Katowice

Title: EMPA, XRD, and Raman characterization of Ag-Bearing Djurleite from the Lubin mine, Lower Silesia, Poland

Author: Krzysztof Szopa, Tomasz Krzykawski, Kamila Banasik, Piotr Król, Sylwia Skreczko, Stefania Andriopoulou Mouteanou, Marta Koziarska

Citation style: Szopa Krzysztof, Krzykawski Tomasz, Banasik Kamila, Król Piotr, Skreczko Sylwia, Andriopoulou Mouteanou Stefania, Koziarska Marta. (2021). EMPA, XRD, and Raman characterization of Ag-Bearing Djurleite from the Lubin mine, Lower Silesia, Poland. "Minerals" (Vol. 11, iss. 5 (2021), art. no. 454), doi 10.3390/min11050454



Uznanie autorstwa - Licencja ta pozwala na kopiowanie, zmienianie, rozprowadzanie, przedstawianie i wykonywanie utworu jedynie pod warunkiem oznaczenia autorstwa.

Article

EMPA, XRD, and Raman Characterization of Ag-Bearing Djurleite from the Lubin Mine, Lower Silesia, Poland

Krzysztof Szopa ^{1,*}, Tomasz Krzykawski ¹, Kamila Banasik ¹, Piotr Król ², Sylwia Skreczko ¹, Stefania Andriopoulou Mouteanou ³ and Marta Koziarska ²

¹ Faculty of Natural Sciences, Institute of Earth Sciences, University of Silesia in Katowice, 41-200 Sosnowiec, Poland; tomasz.krzykawski@us.edu.pl (T.K.); kamila.banasik@us.edu.pl (K.B.); sylwia.skreczko@us.edu.pl (S.S.)

² Institute of Geological Sciences, Polish Academy of Sciences, 00-818 Warsaw, Poland; piotr.krol@twarda.pl (P.K.); m.koziarska@ingpan.krakow.pl (M.K.)

³ Department of Geology, University of Patras, GR-26504 Rio-Patras, Greece; stef.geology@gmail.com

* Correspondence: krzysztof.szopa@us.edu.pl; Tel.: +48-603813074

Abstract: The chalcocite group minerals are widely distributed among different hydrothermally affected rocks, the oxidized zone of copper sulfide deposits, or may be even crystalline from supersaturated volcanic gases. Some of the chalcocite group minerals form the main Cu orebodies. Djurleite (Cu₃₁S₁₆) is a rare member of the chalcocite group, with a very complex structure. The physical and chemical similarities between all members of the group make them almost unidentifiable by macroscopic and microscopic methods. In this study, Ag-bearing djurleite from the Kupferschiefer deposits, Lower Silesia, Poland, is characterized by EMPA (Electron Microprobe Analyses), XRD (X-Ray Diffraction), and Raman spectroscopy. Djurleite from the investigated site has the following general, average chemical formula: Cu_{30.86}Ag_{0.1}Fe_{0.04}S₁₆. The Ag content is up to 0.55 wt.%, while Fe is up to 0.19 wt.%. The presence of djurleite confirms a low-temperature (~90 °C), hydrothermal origin of the Cu-Ag deposit in Kupferschiefer, which is consistent with previously studies. Moreover, the authors believe that Ag-rich djurleite may often be mistaken for Ag-rich chalcocite, which used to be one of the main Ag-bearing minerals in the orebody from the Cu-Ag deposit in the Fore-Sudetic Monocline. However, the confirmation of such a statement requires more samples, which should be studied in detail.

Keywords: djurleite; Lubin; Kupferschiefer; Cu-Ag ore body



Citation: Szopa, K.; Krzykawski, T.; Banasik, K.; Król, P.; Skreczko, S.; Mouteanou, S.A.; Koziarska, M. EMPA, XRD, and Raman Characterization of Ag-Bearing Djurleite from the Lubin Mine, Lower Silesia, Poland. *Minerals* **2021**, *11*, 454. <https://doi.org/10.3390/min11050454>

Academic Editors: Luca Bindi and Nikita V. Chukanov

Received: 15 March 2021

Accepted: 22 April 2021

Published: 26 April 2021

Publisher's Note: MDPI stays neutral with regard to jurisdictional claims in published maps and institutional affiliations.



Copyright: © 2021 by the authors. Licensee MDPI, Basel, Switzerland. This article is an open access article distributed under the terms and conditions of the Creative Commons Attribution (CC BY) license (<https://creativecommons.org/licenses/by/4.0/>).

1. Introduction

Djurleite (space group P2₁/n, a: 2.690, b: 1.575, c: 1.357 nm, and β: 90.13°) is a copper sulfide with the general chemical formula of Cu₃₁S₁₆. It crystallizes with a monoclinic-prismatic symmetry. Djurleite is typically massive in form, but can occur as a thin tabular of prismatic crystals. It is a member of the chalcocite group, and is very similar to chalcocite itself (Cu₂S) in its composition and properties, but the two minerals can be distinguished from each other using X-ray powder diffraction (XRD). Intergrowths and transformations between djurleite, digenite, and chalcocite are common. Moreover, in reflected light, djurleite is less bluish than digenite, and its reflectivity is higher than both digenite and bornite, in air and in oil, respectively. Using polarized light, djurleite is moderately anisotropic, and changes from a strong bluish to a yellowish tint. The polishing- and scratching-hardness of djurleite are almost identical to most of the chalcocite group minerals (e.g., [1]).

Djurleite is widely distributed, but in most cases it is in an accessory phase, without economic use as a copper ore. It is mostly found in the secondary enrichment zones of copper deposits, associated with other copper sulfides, i.e., chalcocite, bornite, chalcopyrite, or digenite.

In this study, Ag-bearing djurleite from the Lubin mine (Figure 1) in Poland is described. It forms a massive orebody associated with bornite and pyrite. Macroscopically, the chalcocite group members are hard or almost impossible to distinguish through both macroscopic and microscopic observations. Additionally, chalcocite and djurleite identification requires XRD or other, much more suitable and sensitive methods.

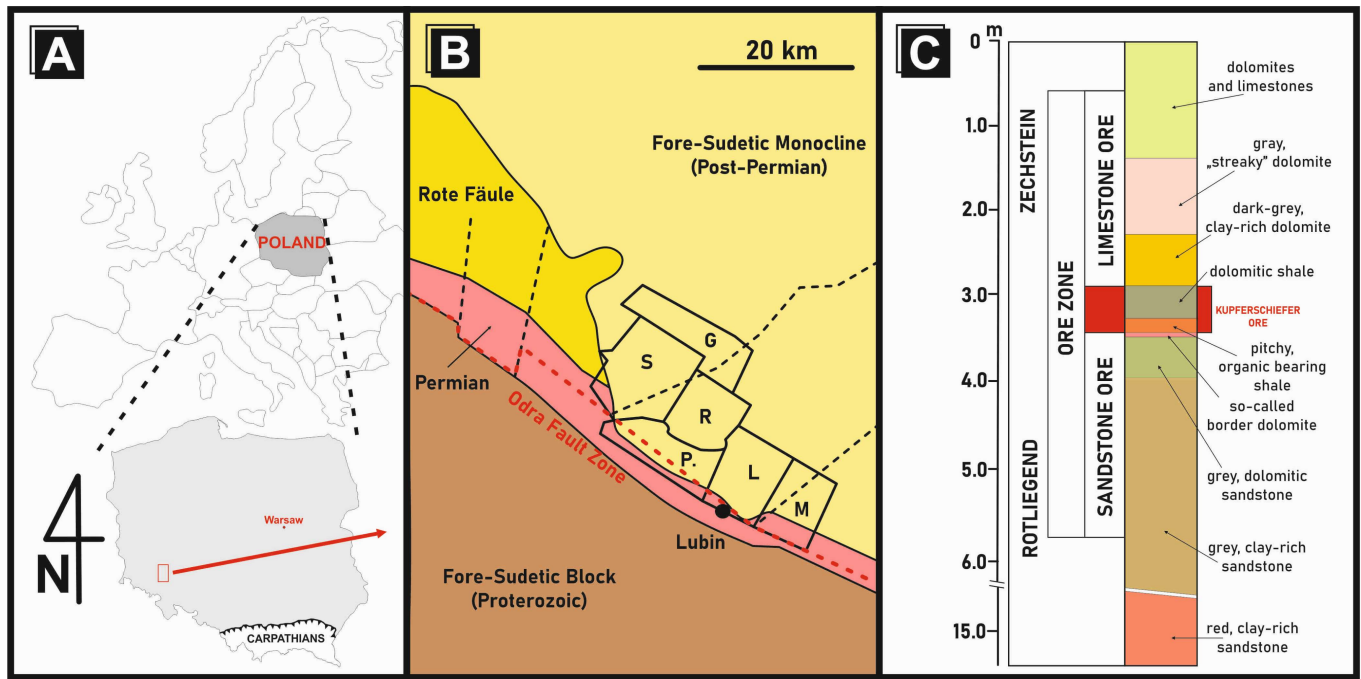


Figure 1. (A) Simplified map of Poland with (B) the Lubin–Sieroszowice Cu–Ag deposits, including the following main mining fields: G—Głogów Deep; S—Sieroszowice; R—Rudna; P—Polkowice; L—Lubin; M—Małomica. Modified after the literature [2], and (C) schematic lithological profile with the Kupferschiefer ore position (based on [3]).

In this paper, we present the mineralogical and compositional features of djurleite (Figure 2) in the Kupferschiefer Unit from Lower Silesia in Poland. Following detailed observations using an optical microscope, back-scattered electron imaging (BSE), XRD, and Raman spectroscopy, these investigations led to the identification of Ag-rich djurleite, which is commonly not recognized during explorations in the mine. Moreover, this is the first detailed characterization of Ag-rich djurleite from the Kupferschiefer Unit in Poland, especially in terms of XRD and Raman spectroscopy.

However, the first report of djurleite from the Cu–Ag deposits on the Fore-Sudetic Monocline was done by Harańczyk and Jarosz [4]. After that, only a few studies from the investigated area included djurleite. Kucha [5] confirmed the optical properties of djurleite and classified this mineral as one of the main Cu minerals in the Kupferschiefer stratum in Poland. Moreover, some chemical data for djurleite, based on EPMA, were previously presented [6,7].

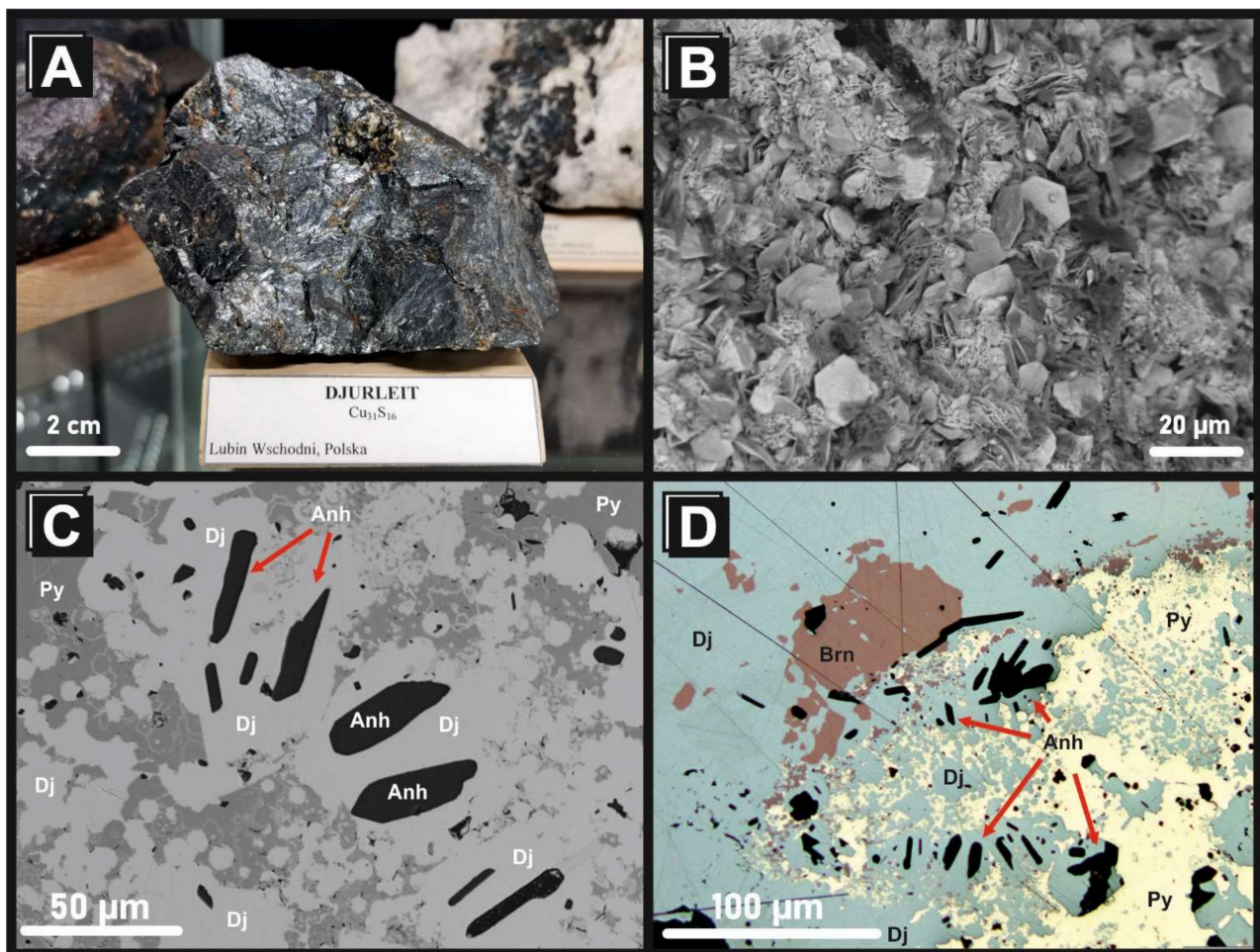


Figure 2. (A) Sample of the djurleite studied (previously identified as chalcocite), from the mineralogical collection of the Earth Sciences Museum, University of Silesia, Katowice, Poland. (B) Crystals of djurleite (back-scattered electron imaging (BSE) image) in a small cavity. (C) BSE image of djurleite (Dj) associated with bornite (Brn) and pyrite (Py). The dark mineral is anhydrite (Anh). (D) The same association in reflected light.

2. Geological Setting

The copper–silver ore mineralization of southwestern Poland occurs in the geological extension of the Kupferschiefer stratum of the Zechstein Basin, which extends from the UK in the west, towards eastern Poland in the east. In Poland, the ore deposits are located in the south-western marginal part of the Fore-Sudetic Monocline and in the North Sudetic Trough (Figure 1B). These two parts are separated by the Fore-Sudetic Block along Middle Odra Fault System in the north, and the Marginal Sudetic Fault in the south. The latest comprehensive geological descriptions of the Kupferschiefer deposit are given by the authors of [8–11].

The pre-Variscan basement of the Fore-Sudetic Monocline is formed by Precambrian to lower Paleozoic metamorphic and Devonian–Carboniferous sedimentary rocks [12]. The basement cover is commonly composed of NE-dipping Permo-Triassic (Cimmerian), Cretaceous (Laramide), and post-Laramide successions. Directly on the crystalline basement, conglomerates, sandstones, and volcanic rocks composed of rhyolites, rhyolitic tuffs, and trachy-basalts of early-Permian (the Lower Rotliegend) appear [3,13]. Conglomerates and brown-red sandstones overlie the volcanic rocks or lie directly on the older basement, and pass upward into white and grey sandstones of the Upper Rotliegend (the so-called Weissliegend, on account of the white color of the sediments). The thickness of the sedimentary Rotliegend succession reaches up to 300 m, whereas the volcanic rocks are up to 1000 m (e.g., [3]).

The ore-deposit series comprise the Weissliiegend sandstones and the lower part of Zechstein, i.e., the Basal Dolomite, Kupferschiefer, and Zechstein Limestone units. Pale-grey, fine- to medium-grained arenitic sandstones of Weissliiegend are formed in fluvial, eolian, and shallow-marine environments, reaching 18 m in thickness on average [8,14]. Locally, Weissliiegend sediments are overlain by up to 30 cm of stratum or lenses of dolomites and limestones of the Basal Limestone Unit, traditionally called the Boundary Dolomite. On the Boundary Dolomite, or directly on the Weissliiegend deposits, copper-bearing shales, traditionally denominated “Kupferschiefer”, occur. Kupferschiefer is composed of clayey shales, laminated marls, or dolomitic marls [2,15,16], rarely silt shales or mud shales [17], rich in organic matter. The thickness is variable, reaching up to 70 cm, but locally the Kupferschiefer is absent in the profile. Copper-bearing shales are overlain by Zechstein Limestone sediments, whose lower part is composed of clayey dolomites (wackstones) and locally of dolomitic limestones (mostly packstones and wackstones) [17]. The Zechstein limestone is up to 110 m thick [8].

The Zechstein limestone is followed in the profile by the Lower Anhydrite and Oldest Halite series [9]. The upper part of the Zechstein succession is developed in the form of classic evaporate cyclothemes, including limestones, dolomites, anhydrites, rock salts, and clayey shales. This is followed by Triassic sandstones and clayey shales. The Cretaceous deposits discordantly overlie Triassic rocks and are covered by Eocene–Oligocene sandstones, Miocene clays, sands, and gravels, and finally Quaternary sediments.

The copper–silver deposits penacordantly cross-cut the upper-Rotliegend and Zechstein strata. Both vertical and horizontal zonation of metals and ore minerals are present [18]. The ore deposit occurs around the oxidized barren zone rich in hematite, the so-called Rote Fäule (e.g., [19]), which marks the redox interface. This is followed by the Cu-rich zone, with ore minerals changing from chalcocite, bornite, to chalcopyrite, and then by commonly overlapping lead and zinc zones with the former on the proximal side. Finally, the barren, Fe²⁺ zone occurs, containing mostly pyrite. Between the ore-mineralized and Rote Fäule zone, there is a transition zone in which sulfide remnants are present within the hematite-bearing rocks [11], where Au, Pt, and Pd mineralization are found in either the shale or sandstone (e.g., [18,20,21]).

Mineralogy and Material

Until recently, more than 150 mineral phases were described from the studied area (e.g., [19–25]). Chalcocite is the dominant mineral in the copper ore, locally comprising the massive ore, reaching up to 90% of the volume of the rock. Other minerals forming the copper ore include bornite, chalcopyrite, digenite, covellite, galena, sphalerite, pyrite, tennantite, and tetrahedrite [16,20]. The main ore minerals belong to either the chalcocite-digenite group, with chalcocite, digenite, covellite, and others, or to the Cu-Fe-S group, with bornite, chalcopyrite, idaite, mooihoekite, and others, which are more rarely present. Galena and sphalerite comprise the main lead and zinc sulfides, respectively.

The following forms of ore mineralization are presented [8,22]: disseminated, nests, veins and veinlets, lenses, bands, and massive forms. The former is prevalent throughout the whole ore body. In the copper-bearing shales, disseminated and veinlet-hosted mineralization is the most common. Within the sandstones and conglomerates, ore minerals occur in the form of pore fillings, vein-type, replacement of cements, diagenetic pyrite, and some feldspar grains. Disseminated and nest- and vein-type mineralization occur in carbonates.

The investigated sample was taken from the Earth Sciences Museum, University of Silesia in Katowice, Poland. The studied material is stored in the mineralogical collection at the Museum, number WNOZ/M/2/227 (Figure 2A). Before the examination of the investigated sample, this specimen was classified as chalcocite. This previous investigation was done based on macroscopic observation.

The sample of djurleite that was studied was from the Lubin mine (Figure 1B), which is located on the northern part of the Lubin town, in Lower Silesia. The Lubin mine is the oldest mine in the so-called Polish Copper Belt in Poland. In the mine, the Lubin–Małomice

deposit is explored, and is characterized by intensive tectonic displacements within the orebody, especially in its south-west part—the deposit here is found at a shallow depth, under loose Cenozoic sediments.

3. Analytical Techniques

3.1. Microscopy

Petrographic analyses of thin sections and polished slabs were undertaken at the Institute of Earth Sciences, Faculty of Natural Sciences, University of Silesia in Katowice using an Olympus BX-51 microscope to identify the djurleite, as well as to characterize its association. The petrographic observations were used to select representative samples for BSE and subsequent electron probe micro-analysis, as well as other structural and geochemical analyses.

3.2. Electron Probe Micro-Analyses (EPMA)

Microprobe analyses of the ore minerals from the studied sample were carried out at the Inter-Institutional Laboratory of Microanalyses of Minerals and Synthetic Substances, Warsaw, using a CAMECA SX-100 electron microprobe. The analytical conditions employed an accelerating voltage of 15 keV, a beam current of 20 nA, counting times of 4 s for the peak and background, and a beam diameter of 1–5 μm . The universal correction procedure for EPMA was done based on the literature [26]. The reference materials, analytical lines, diffracting crystals, average detection limits (in wt.%; for all of the analyzed points) and uncertainties were as follows: chalcopyrite—S ($K\alpha$, PET, 0.05), chalcopyrite—Cu ($K\alpha$, LIF, 0.2), chalcopyrite—Fe ($K\alpha$, LIF, 0.1), rutile—Ti ($K\alpha$, PET, 0.05), GaAs—As ($L\alpha$, TAP, 0.9), CoO—Co ($K\alpha$, LIF, 0.08), sphalerite—Zn ($K\alpha$, LIF, 0.25), PbS—Pb ($M\alpha$, PET, 0.25), Bi₂Se₃—Se ($L\alpha$, TAP, 0.03, 0.02), rodonite—Mn ($K\alpha$, LIF, 0.1), Au-SPI—Au ($L\alpha$, LPET, 0.15), and Ag₂Te—Ag ($L\alpha$, LPET, 0.05).

3.3. Raman Spectroscopy

The Raman spectrum of the studied mineral phases was recorded on a WITec alpha 300R Confocal Raman Microscope (at the Institute of Earth Sciences, Faculty of Natural Sciences, University of Silesia in Katowice), equipped with an air-cooled solid laser at 532 nm and 488 nm using a CCD camera operating at $-61\text{ }^{\circ}\text{C}$. The laser radiation was coupled to a microscope through a single-mode optical fiber with a diameter of 3.5 μm . An air Zeiss LD EC Epiplan-Neofluar DIC 100/0.75NA objective was used. Raman scattered light was focused using a broad band single mode fiber with an effective Pinhole size of about 30 μm and a monochromator with a 600 mm^{-1} grating. The integration and accumulation time depended on the analyzed phase, and ranged from 3 s to 20 s, and from 10 to 45 scans, respectively. The monochromator was calibrated using the Raman scattering line of a silicon plate (520.7 cm^{-1}).

3.4. X-ray Diffraction (XRD)

XRD characterization was also carried out in the Institute of Earth Sciences, Faculty of Natural Sciences, University of Silesia in Katowice. The djurleite fragments were ground manually using an agate mortar for 5 min. In order to correct the peak positions on the XRD pattern due to the sample displacement shift, small amounts of alpha-Quartz (NIST SRM 1878b) powder were mixed with the sample, as an internal standard. Finally, standard zero background Si sample holders with a cavity were filled with powder. X-ray diffraction analyses (XRD) were assessed with the aid of a Panalytical X'Pert PRO PW 3040/60 X-ray diffractometer (Almelo, Holland), equipped with an X-ray tube (Cu $K\alpha 1$ source radiation, $\lambda = 1.540598\text{ \AA}$). To reduce the $K\beta$ radiation, a Ni-filter was used. The diffracted radiation was measured by means of an X'Celerator detector, with an active length of $2.122^{\circ}2\theta$ for the silicon strip. The measurement parameters were acceleration voltage: 40 kV; filament current: 40 mA; counting time: 300 s; start angle: $5^{\circ}2\theta$; end angle: $65^{\circ}2\theta$; step size: $0.017^{\circ}2\theta$; and the scan speed was: $0.0035^{\circ}/\text{s}$. The analysis of the

collected data was carried out by means of the X'Pert HighScore Plus+ Software (version 4.9, Malvern-Panalytical, Almelo, The Netherlands) using the ICSD PDF4+ database (version 2018). The cell parameters of the djurleite were calculated using the Rietveld Method. The djurleite peak parameters obtained in this study are in Table 1. All detailed XRD data are presented in Tables S1 and S2.

Table 1. Djurleite peak parameters obtained from the measured diffraction pattern (XRD).

d-Spacing (Å)	Relative X-ray Intensity (%)	d-Spacing (Å)	Relative X-ray Intensity (%)
6.0497	1.5	2.5197	12.0
5.6502	1.2	2.4820	9.7
5.0709	1.2	2.4196	12.3
4.7772	1.8	2.3919	64.1
4.5970	2.1	2.3202	6.3
4.4589	2.0	2.2923	6.2
4.2910	5.3	2.2853	6.7
4.1279	1.2	2.2674	4.8
3.9051	7.3	2.2348	3.7
3.7649	11.8	2.1934	4.5
3.6496	4.0	2.1443	6.7
3.5910	7.4	2.1111	4.4
3.4780	3.3	2.0721	6.6
3.3960	29.0	2.0659	6.4
3.2854	12.3	2.0481	6.4
3.1967	14.6	1.9896	5.7
3.1080	11.8	1.9590	78.6
3.0407	15.4	1.9372	7.1
3.0154	15.8	1.8730	100.0
2.9448	6.7	1.8324	2.8
2.8953	13.6	1.7809	3.7
2.8713	12.4	1.7681	2.7
2.8380	13.7	1.7541	1.8
2.8165	11.3	1.7214	2.0
2.7878	6.4	1.6930	21.8
2.7378	6.0	1.6829	14.4
2.7103	9.2	1.6470	9.1
2.6925	10.5	1.6460	8.1
2.6581	16.5	1.5779	0.2
2.6236	3.9	1.5398	0.9
2.6012	8.3	1.5166	5.3
2.5596	11.9	1.4654	1.8

4. Results and Discussion

4.1. Mineralogy of Ag-Rich Djurleite from the Kupferschiefer Deposit, Lower Silesia, Poland

The investigated sample represents the grey, massive, and compact fragment of the orebody (Figure 2A), with a characteristic metallic luster. Sporadically, small veins with platy Cu_2S (djurleite?) crystals up to tens of millimeters were noted (Figure 2B). In such a case, small, up to 20 μm in size, automorphic crystals of both phases of djurleite and anhydrite occur in empty microdruses. Anhydrite crystals (Figure 2C,D) are rare, where its content is less than 0.1 wt.% of the total investigated sample mass. Djurleite is grey to blueish grey in reflected light (Figure 2D). BSE imaging revealed local banded colloform-like textures, which are represented by bornite, and pyrite lamellae overgrown.

The djurleite from the investigated site can be characterized by the following general, average formula: $\text{Cu}_{30.86}\text{Ag}_{0.1}\text{Fe}_{0.04}\text{S}_{16}$. The Ag content is up to 0.55 wt.%, while the Fe is up to 0.19 wt.% (Table 2). Electron microprobe analyses did not reveal any other important elemental substitution in the djurleite composition. Bornite is the second, slightly enriched Ag phase. The average Ag content in this mineral is 0.35 wt.%, while the Fe content is up to 11.25 wt.% (Table S3).

Table 2. Selected representative electron microprobe analyses of djurleite from the Lubin mine, Poland. Crystal chemical formulae recalculated on basis of 16 S²⁻.

Compound	an.1	an.2	an.3	an.4	an.5	an.6	an.7	an.8	an.9	an.10	an.11	an.12	an.13	an.14	an.15	an.16
Ag (wt.%)	0.49	0.42	0.44	0.47	0.42	0.41	0.36	0.48	0.41	0.37	0.45	0.55	0.42	0.38	0.47	0.45
Fe	b.d.l.	b.d.l.	b.d.l.	b.d.l.	b.d.l.	b.d.l.	b.d.l.	0.23	0.19	0.31	b.d.l.	b.d.l.	b.d.l.	b.d.l.	b.d.l.	0.19
Cu	79.78	79.90	80.51	79.80	76.61	79.47	79.90	79.57	79.83	80.28	78.83	79.15	79.48	79.74	80.21	78.40
S	20.93	20.86	21.00	20.84	20.01	20.80	20.82	20.85	20.93	21.04	20.99	20.71	20.77	20.81	20.96	20.55
Total	101.21	101.18	101.95	101.11	97.04	100.69	101.08	101.12	101.35	101.99	100.26	100.40	100.67	100.93	101.64	99.60
Ag (apfu)	0.11	0.10	0.10	0.11	0.10	0.09	0.08	0.11	0.09	0.08	0.10	0.13	0.10	0.09	0.11	0.10
Fe	-	-	-	-	-	-	-	0.10	0.08	0.13	-	-	-	-	-	0.09
Cu	30.78	30.92	30.96	30.91	30.91	30.85	30.98	30.82	30.80	30.81	30.33	30.86	30.89	30.94	30.90	30.80
S	16	16	16	16	16	16	16	16	16	16	16	16	16	16	16	16

b.d.l.—below detection limit; an—analyze no.

For the refining procedure of the analyzed djurleite structure, the reference pattern with the number 04-007-1283 in the ICDD PDF4 + database (2018) was used. The data contained in this file were calculated on the basis of the work by Evans H.T., Jr. [27], for the djurleite specimen from the Ozark Lead Co. mine, Sweetwater, Missouri, USA. For this djurleite, the following structural parameters were shown: space group number 14 (P21/n), $a = 26.897 \text{ \AA}$, $b = 15.745 \text{ \AA}$, $c = 13.565 \text{ \AA}$, and $\beta = 90.13^\circ$. For the investigated djurleite, a very good match for all reflections of the XRD pattern to the peaks of the reference pattern was observed (Figure 3); however, no reflections from the admixture of chalcocite were recorded. The performed Rietveld refinement allowed for achieving the following agreement indices: $Re = 1.376$, $Rp = 2.425$, $Rwp = 3.459$, and $GoF = 6.320$. The structural parameters of the analyzed djurleite were as follows: $a = 26.885(4) \text{ \AA}$, $b = 15.706(2) \text{ \AA}$, $c = 13.533(2) \text{ \AA}$, and $\beta = 89.909(2)^\circ$.

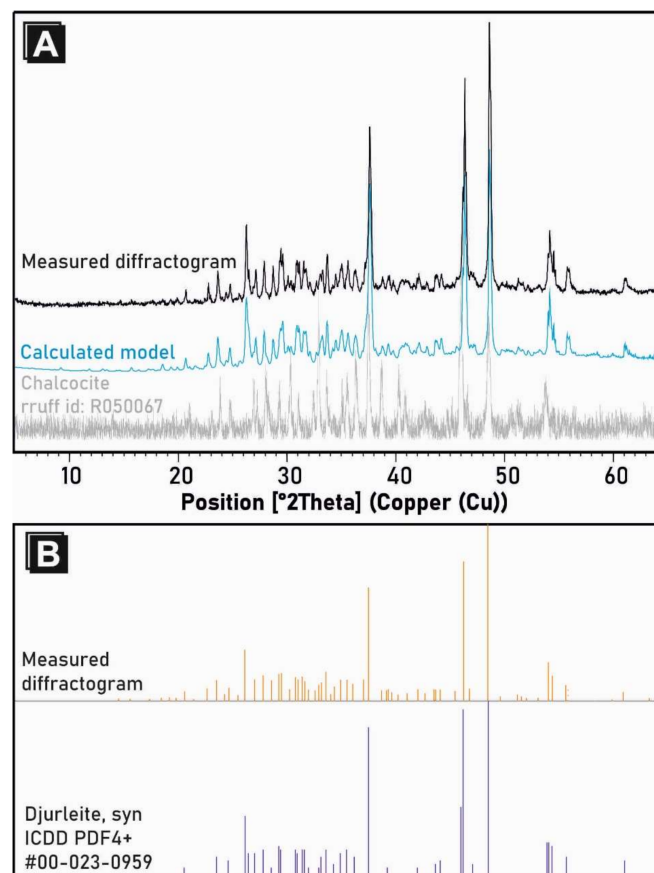


Figure 3. (A) XRD pattern of the investigated djurleite compared with both calculated models (by the Rietveld method) and chalcocite (a basic standard). (B) List of all peaks from the characterized sample and a typical djurleite (ICDD, PDF4+ standard, #04-007-1283 reference code).

The obtained Raman spectra of the identified phases are shown in Figure 4 (the investigated djurleite is compared with a basic chalcocite standard). The Raman spectra of djurleite are characterized by a broad band at 294 cm^{-1} , which shifted to lower wave numbers than the chalcocite, with a band at 300 cm^{-1} [28]. Considerable enlargement of the main broad band, as well as slight increases of intensity in the lower wave number positions, suggest the presence of an admixture of other metals in the djurleite structure. The EMPA data show a minor presence of Ag in its chemical composition. Silver atoms are larger and heavier than copper, which is reflected in the bond length between the sulfur and metal in the crystal structure [28]. The discussed Raman spectrum does not show the typical spectra for silver sulfide, with a sharp peak at 147 cm^{-1} , corresponding to an Ag lattice vibration mode, but is characteristic for the copper sulfide Cu-S-Cu symmetric stretching mode, showing a shift depending on the ratio between Ag and Cu, being in line with the dominant Cu atoms in the djurleite structure [28]. Against the main enlargement band in the region of $320\text{--}350\text{ cm}^{-1}$, this can show the character of the phonon mode for a variable Cu_{2-x}S system [29]. A low intensity broad band at 472 cm^{-1} assigned to a S-S stretching mode position confirms the chemo-structural similarity inside the copper sulfide system for djurleite, where the discussed vibrations are closer to the chalcocite stretching mode at 471 cm^{-1} than to covellite at 474 cm^{-1} , respectively [30].

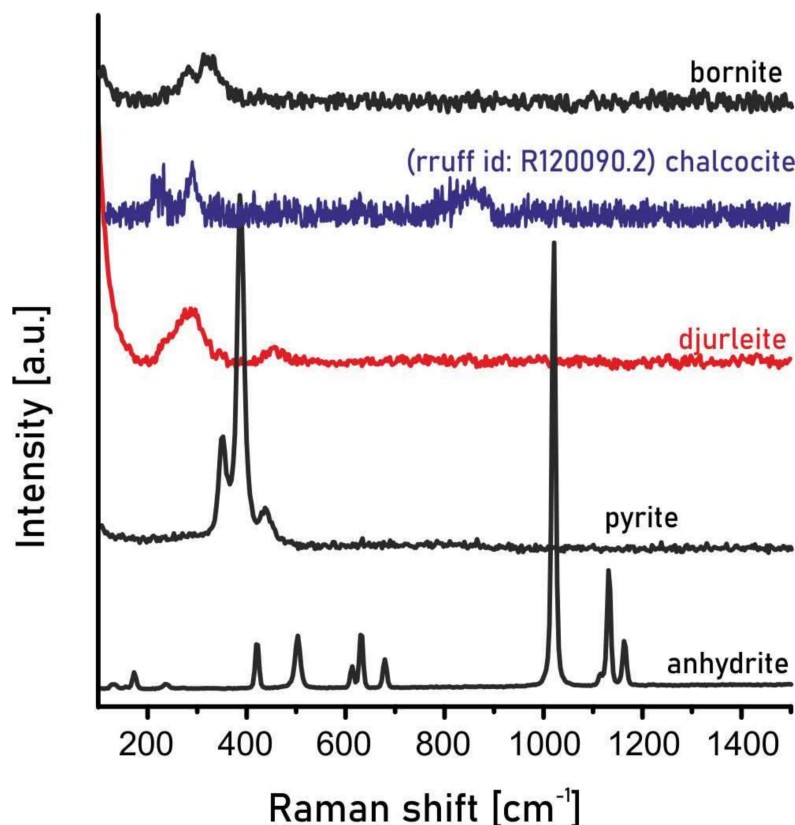


Figure 4. Raman shifts of all minerals from the investigated sample from the Lubin mine, Poland. A basic chalcocite standard is added for comparison.

Additionally, the spectra of anhydrite, pyrite, and bornite were obtained (Figure 4). In the Raman spectrum of anhydrite, the following bands were distinguished: 123 cm^{-1} , 151 cm^{-1} , 168 cm^{-1} , 230 cm^{-1} , 268 cm^{-1} , 415 cm^{-1} , 499 cm^{-1} , 609 cm^{-1} , 626 cm^{-1} , 675 cm^{-1} , 1017 cm^{-1} , 1111 cm^{-1} , 1127 cm^{-1} , and 1158 cm^{-1} , while for pyrite, the characteristic vibrations bands at 347 cm^{-1} , 381 cm^{-1} , and 432 cm^{-1} are visible. The above described Raman spectra are typical for these minerals, and they not differ from the literature data [31–37]. The obtained Raman spectrum for bornite (which was confirmed by EMPA data) shows two wide bands in the region between 200 and 400 cm^{-1} , which

corresponds to the bands visualized in all of the available bornite Raman spectra (among others, the RRUFF Database; [35]).

4.2. Formation Conditions of Ag-Djurleite

The formation of the Cu-bearing zone in the Lubin–Sieroszowice Cu–Ag deposits was estimated on the basis of vitrinite reflectance in order to determine the temperature conditions, and was in a range from 65 to 110 °C [24,38–41]. However, it must be taken into consideration that the temperature conditions forming the oxidative alteration by oxidizing fluids was up to 135 °C [8,39–43]. The estimated maximum temperatures reflected the temperatures of hydrothermal fluids responsible for both secondary oxidation and the Cu mineralization [38,39,42]. Furthermore, based on the assumption that monoclinic chalcocite is the main ore mineral in the deposit, Piestrzyński [22] suggested that Cu-bearing mineralization formed at a temperature less than 103.5 °C. However, the phase relationships of the copper sulfides have been studied extensively. Monoclinic chalcocite converts to a high-temperature hexagonal polymorph at 103 °C, and the upper limit of stability of djurleite is 93 °C (Figure 5) [26,43–46].

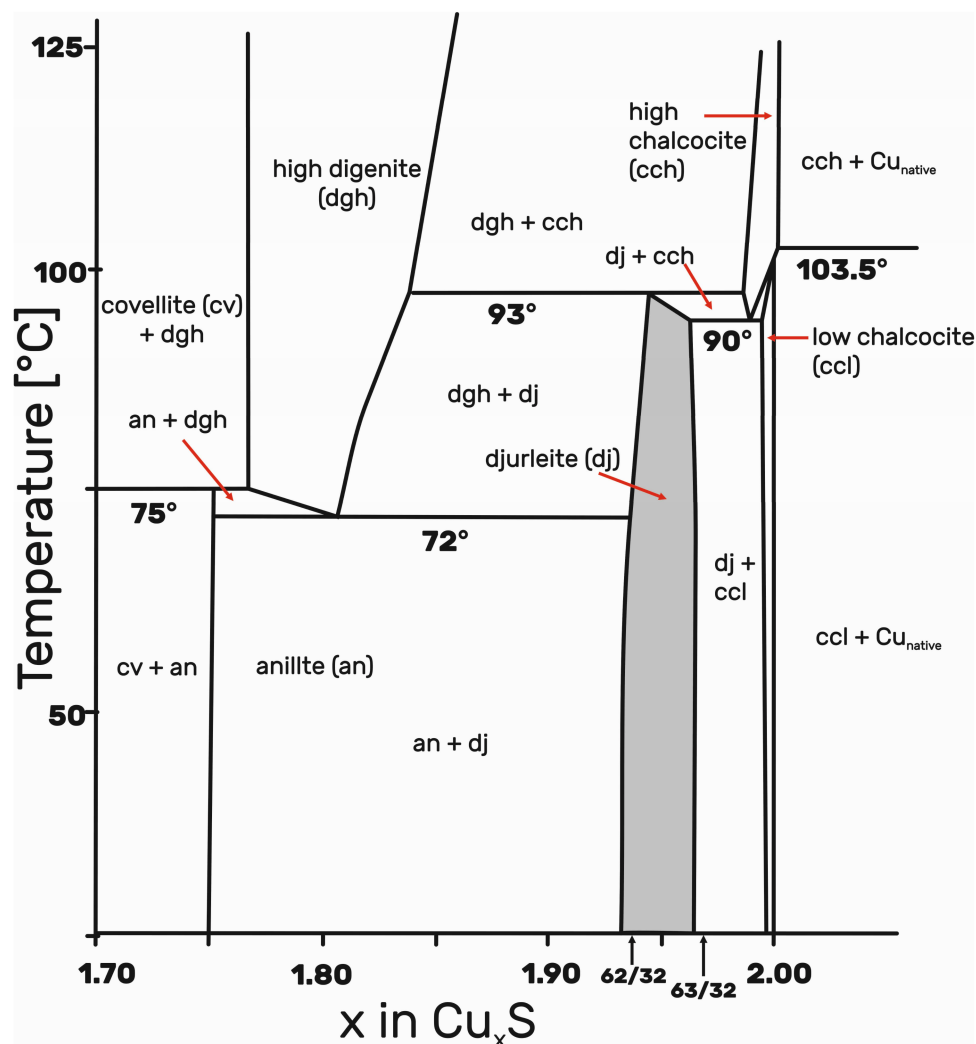


Figure 5. Phase diagram for the Cu–S system in the low temperature region near Cu₂S from the literature [27]. The single djurleite area is shaded.

Experiments on the synthesis of copper sulfides by nonhydrolytic sol–gel are often applied. Precisely controlled synthesis of different Cu_xS polymorphs, including, e.g., chalcocite (α and β), djurleite, low digenite, and covellite, have confirmed that djurleite

is a low temperature phase. The solvo-thermal reactions of mono copper chloride and hexamethyldisilathiane in acetonitrile from 70 °C to 130 °C for seven days yield djurleite. Similar results, but with less crystalline djurleite, have been obtained in chloroform at 70 °C (e.g., [27,46]). Moreover, the conversion of chalcocite to djurleite, as well as digenite to covellite, have been observed, similarly to the observations of low-temperature chalcocite alteration in the Lubin and Rudna mines [46].

In some cases, the metasomatic transformation of chalcocite and bornite by native silver, silver amalgams, and stromeyerite most likely indicates that the Ag-bearing mineralization associated with, e.g., cupropearceite, post-dated the main process of the formation of Cu-bearing mineralization [24].

5. Conclusions

In this paper, we present, firstly, a geochemical overview of the Ag-bearing djurleite from the Lubin Mine, Kupferschiefer Unit, containing numerous Cu- and Ag-rich minerals (mostly sulfides) in Poland, one of the world's major producers of copper and silver. The djurleite in this study has a constant content of Ag, which is ~0.5 wt.%. In the Lubin mine, Ag-bearing djurleite is associated with bornite; pyrite; and, rarely, anhydrite. Chalcocite was not found in the studied sample.

The chemical composition of djurleite in this study is similar to other in previously published data. However, the average content of Ag in the studied djurleite is higher than that published by the authors of [7] (mean Ag content = 0.33 wt.%) and [6] (mean Ag content = 0.1 wt.%).

The djurleite is easily identified by XRD and Raman spectroscopy, showing its characteristic peaks and vibration bands, respectively. The presented data can be helpful as reference data, which can be used to distinguish other minerals from the chalcocite group, especially chalcocite itself. Extended studies on the main Cu- and Ag-orebody samples from different parts of the Kupferschiefer strata could conclude that djurleite could be more common than chalcocite.

The investigated sample, and its mineralogy, confirmed the low temperature (~90 °C) origin of the orebody, which is consistent with the previously published data, based on both experiments and field observations (e.g., [26,43–46]).

Supplementary Materials: The following are available online at <https://www.mdpi.com/article/10.3390/min11050454/s1>, Table S1: Relevant parameters of djurleite (structure and profile data); Table S2: The occupancy, atomic fract. coordinates and biso for djurleite; Table S3: Selected representative electron microprobe analyses of bornite from the Lubin mine, Poland. Crystal chemical formulae recalculated on basis of 4 S²⁻.

Author Contributions: Conceptualization, K.S.; methodology, K.S., T.K. and K.B.; formal analysis, S.A.M. and M.K.; investigation, all of the authors.; writing—original draft preparation, K.S., P.K. and S.S.; writing—review and editing, all authors; visualization, K.S., T.K., and K.B., mineral calculations S.A.M. and M.K. All authors have read and agreed to the published version of the manuscript.

Funding: Krzysztof Szopa acknowledges the financial support from the Institute of Earth Sciences ("Małe Projekty Badawcze finansowane z Rezerwy Dyrektora INoZ"), Faculty of Natural Sciences, University of Silesia in Katowice, Poland.

Institutional Review Board Statement: Not Applicable.

Informed Consent Statement: Not Applicable.

Data Availability Statement: Not Applicable.

Acknowledgments: The authors thank Beata Marciniak-Maliszewska for her help during the microprobe analyses, and Ashley P. Gumsley for his help in improving the English of the manuscript. The manuscript benefited from the comments of four anonymous reviewers. Authors are very grateful for their work.

Conflicts of Interest: The authors declare no conflict of interest. The funders had no role in the design of the study; in the collection, analyses, or interpretation of data; in the writing of the manuscript, or in the decision to publish the results.

References

1. Morimoto, N. Djurleite, a new copper sulfide mineral. *Mineral. J.* **1962**, *3*, 338–344. [[CrossRef](#)]
2. Oszczepalski, S.; Speczik, S.; Małecka, K.; Chmielewski, A. Prospective copper resources in Poland. *Gospod. Surowcami Miner.* **2016**, *32*, 5–30. [[CrossRef](#)]
3. Banaś, M.; Salamon, W.; Piestrzyński, A.; Mayer, W. Replacement phenomena of terrigenous minerals by sulphides in copper-bearing Permian sandstones in Poland. In *Ore Genesis—The State of the Art*; Amstutz, G.C., Ed.; Springer: Berlin/Heidelberg, Germany, 1982; pp. 3–9.
4. Harańczyk, C.; Jarosz, J. Ore minerals from copper deposit in Fore-Sudetic Monocline. *Rudy I Met. Niżel* **1973**, *18*, 493–502. (In Polish)
5. Kucha, H. Mineralogy and geochemistry of the Lubin-Sieroszowice orebody. *Biuletyn Państwowego Inst. Geol.* **2007**, *423*, 77–94. (In Polish with English Summary).
6. Oszczepalski, S.; Chmielewski, A.; Speczik, S. Variability of ore mineralization in the north-west-trending extension of the Lubin–Sieroszowice deposit. *Biuletyn Państwowego Inst. Geol.* **2017**, *468*, 109–142. (In Polish with English Summary). [[CrossRef](#)]
7. Mikulski, S.Z.; Oszczepalski, S.; Sadłowski, K.; Chmielewski, A.; Małek, R. Trace Element Distributions in the Zn-Pb (Mississippi Valley-Type) and Cu-Ag (Kupferschiefer) Sediment-Hosted Deposits in Poland. *Minerals* **2020**, *10*, 75. [[CrossRef](#)]
8. Borg, G.; Piestrzyński, A.; Bachman, G.H.; Puttmann, W.; Walther, S.; Fidler, M. An overview of the European Kupferschiefer deposits. In *Geology and Genesis of Major Copper Deposits and Districts of the World: A Tribute to Richard, H. Sillitoe*, 1st ed.; Hedenquist, J.W., Camus, F., Eds.; Society of Economic Geologists, Special Publication: Littleton, CO, USA, 2012; Volume 16, pp. 455–486.
9. Jowett, E.C. Genesis of Kupferschiefer Cu-Ag deposits by convective flow of Rotliegendes brines during Triassic rifting. *Econ. Geol.* **1986**, *81*, 1823–1837. [[CrossRef](#)]
10. Oszczepalski, S. Origin of the Kupferschiefer polymetallic mineralization in Poland. *Miner. Depos.* **1999**, *34*, 599–613. [[CrossRef](#)]
11. Vaughan, D.J.; Sweeney, M.; Diedel, G.F.R.; Harańczyk, C. The Kupferschiefer: An overview with an appraisal of the different types of mineralization. *Econ. Geol.* **1989**, *84*, 1003–1027. [[CrossRef](#)]
12. Wierzchowska-Kicułowa, H. Charakterystyka geologiczna podłoża permu obszaru przedsudeckiego. *Geol. Q.* **1987**, *31*, 515–516. (In Polish)
13. Juroszek, C.; Kłapciński, J.; Sachański, M. Wulkanity dolnego permu południowej części Monokliny Przedsudeckiej i Perykliny Żar. *Ann. Soc. Geol. Pol.* **1981**, *51*, 517–546. (In Polish)
14. Nemeč, W.; Porebski, S.J. Sedimentary environment of the Weissliegendes sandstone in Fore-Sudetic monocline. In *Proceedings of the SCEP-Proceedings, International Symposium on Central European Permian*, Jabłonna, Poland, 27–29 April 1979; Pakulska, Z., Ed.; Geological Institute: Warsaw, Poland, 1981; pp. 273–293.
15. Oszczepalski, S.; Rydzewski, A. Paleogeography and sedimentary model of the Kupferschiefer in Poland. *Lect. Not. Earth Sci.* **1987**, *10*, 189–205.
16. Oszczepalski, S.; Speczik, S.; Zieliński, K.; Chmielewski, A. The Kupferschiefer Deposits and Prospects in SW Poland: Past, Present and Future. *Minerals* **2019**, *9*, 592. [[CrossRef](#)]
17. Peryt, T.M.; Oszczepalski, S. Stratygrafia serii złożowej. In *Monografia KGHM Polska Miedź S.A.; Piestrzyński, A., Ed.; KGHM Cuprum Sp. z o.o.: Lubin, Poland, 2007; pp. 108–111. (In Polish)*
18. Pieczonka, J.; Piestrzyński, A.; Sawłowicz, Z. The sediment hosted copper silver deposits in the Lubin–Głogów mining district (Poland). In *Proceedings of the Digging Deeper, Joint 9th Biennial SGA-SEG Meeting*, Dublin, Ireland, 20–23 August 2007; Sass-Gustkiewicz, M., Sawłowicz, Z., Eds.; Rafael: Kraków, Poland, 2007; pp. 7–23.
19. Oszczepalski, S. Kupferschiefer in southwestern Poland. Sedimentary environments, metal zoning, and ore controls. In *Sediment-Hosted Stratiform Copper Deposits*; Boyle, R.W., Brown, A.C., Jowett, E.C., Kirkham, R.V., Eds.; Geological Association of Canada Special Paper; Geological Association of Canada: Waterloo, ON, Canada, 1989; pp. 571–600.
20. Piestrzyński, A.; Sawłowicz, Z. Exploration for Au and PGE in the Polish Zechstein copper deposits (Kupferschiefer). *J. Geochem. Explor.* **1999**, *66*, 17–25. [[CrossRef](#)]
21. Pieczonka, J.; Piestrzyński, A. Minerality kruszcowa złoża rud miedzi na monoklinie przedsudeckiej i ich znaczenie dla genezy. *Gosp. Sur. Miner.* **2006**, *22*, 187–202. (In Polish with English Abstract).
22. Piestrzyński, A. Okruszcowanie. In *Monografia KGHM Polska Miedź S.A.; Piestrzyński, A., Ed.; KGHM Cuprum Sp. z o.o.: Lubin, Poland, 2007; pp. 232–282. (In Polish)*
23. Pieczonka, J. *Factors Controlling Distribution of Ore Minerals within Copper Deposit, Fore-Sudetic Monocline, SW Poland*; Wyd. AGH: Kraków, Poland, 2011; pp. 1–195. (In Polish)
24. Kozub-Budzyń, G.A.; Piestrzyński, A. The first occurrence of cupropearceite in the Kupferschiefer deposit, Lubin mine, SW Poland. *Geol. Q.* **2018**, *62*, 319–326. [[CrossRef](#)]
25. Kucha, H. Geochemistry of the Kupferschiefer, Poland. *Geol. Rundschau* **1990**, *79*, 387–399. [[CrossRef](#)]
26. Pouchou, J.L.; Pichoir, F. “PAP”, *Procedure for Improved Quantitative Microanalysis. Microbeam Analysis Proc.*; Armstrong, J.T., Ed.; San Francisco Press: San Francisco, CA, USA, 1985; pp. 104–106.

27. Evans, H.T. The crystal structures of low chalcocite and djurleite. *Z. Krist. Cryst. Mater.* **1979**, *150*, 299–320. [[CrossRef](#)]
28. De Caro, T.; Caschera, D.; Ingo, G.M.; Calandra, P. Micro-Raman innovative methodology to identify Ag–Cu mixed sulphides as tarnishing corrosion products. *J. Raman Spectrosc.* **2016**, *47*, 852–859. [[CrossRef](#)]
29. Hurma, T.; Kose, S. XRD Raman analysis and optical properties of CuS nanostructured film. *Optik* **2016**, *127*, 6000–6006. [[CrossRef](#)]
30. Santos, C.J.; Mayen, H.S.A.; Coronel, H.J.J.; Mejia, R.R.; Castanedo, P.R.; Torres, D.G.; Jimenez, S.S. Characterization of CuxS thin films obtained by CBD technique at different annealing temperatures. *Chalcogenide Lett.* **2012**, *9*, 85–91.
31. Potter, R.W. An electrochemical investigation of the system copper-sulfur. *Econ. Geol.* **1977**, *72*, 1524–1542. [[CrossRef](#)]
32. Buzgar, N.; Buzatu, A.; Sanislav, I.V. The Raman study on certain sulfates. *Al. I. Cuza* **2009**, *55*, 5–23.
33. Liu, Y.; Wang, A.; Freeman, J.J. Raman, MIR, and NIR spectroscopic study of calcium sulfates: Gypsum, bassanite, and anhydrite. In *Mars Analogs Sulfates and Sulfides Posters, Proceedings of the 40th Lunar and Planetary Science Conference, the Woodlands, Texas, TX, USA, 23–27 March 2009*; Lunar and Planetary Institute: Houston, Texas, TX, USA, 2009; p. 2128.
34. White, S.N. Laser Raman spectroscopy as a technique for identification of seafloor hydrothermal and cold seep minerals. *Chem. Geol.* **2008**, *259*, 240–252. [[CrossRef](#)]
35. Kostudis, S.; Kutschke, H.M.; Pollmann, K. Micro-Raman spectroscopic imaging of copper ores. In *Proceedings of the Conference on Raman and Luminescence Spectroscopy in the Earth Sciences (CORALS-2013)*, Vienna, Austria, 3–6 July 2013; pp. 61–62.
36. Yuan, X.; Zheng, H. In situ Raman spectroscopic studies of FeS₂ pyrite up to 675 K and 2100 MPa using a hydrothermal diamond anvil cell. *Mineral. Mag.* **2015**, *79*, 1–10. [[CrossRef](#)]
37. Kleppe, A.; Jephcoat, A. High-pressure Raman spectroscopic studies of FeS₂ pyrite. *Mineral. Mag.* **2004**, *68*, 433–441. [[CrossRef](#)]
38. Kotarba, M.J.; Oszczepalski, S.; Sawłowicz, Z.; Speczik, S.; Więclaw, D. Materia organiczna i jej rola w procesach złóżotwórczych. In *Monografia KGHM Polska Miedź S.A.*; Piestrzyński, A., Ed.; KGHM Cuprum Sp. z o.o.: Lubin, Poland, 2007; pp. 138–144. (In Polish)
39. Speczik, S.; Oszczepalski, S.; Nowak, G.; Karwasiecka, M. Kupferschiefer—A hunt for new reserves. *Biul. Państwowego Inst. Geol.* **2007**, *42*, 173–188, (In Polish with English Summary).
40. Oszczepalski, S.; Nowak, G.J.; Bechtel, A.; Żák, K. Evidence of oxidation of the Kupferschiefer in the Lubin-Sieroszowice deposit: Implications for Cu-Ag and Au-Pt-Pd mineralization. *Geol. Q.* **2002**, *46*, 1–23.
41. Kosakowski, P.; Markiewicz, A.; Kotarba, M.J.; Oszczepalski, S.; Więclaw, D. The timing of ore mineralization based on thermal maturity modelling of Kupferschiefer strata and its relation to tectonics of southern part of Fore-Sudetic Monocline (SW Poland). *Biul. Państwowego Inst. Geol.* **2007**, *423*, 139–150, (In Polish with English Summary).
42. Roseboom, E.H. An investigation of the system Cu-S and some natural copper sulfides between 25 degrees and 700 degrees C. *Econ. Geol.* **1966**, *61*, 641–672. [[CrossRef](#)]
43. Mathieu, H.J.; Rickert, H. Elektrokemisch-thermodynamische Untersuchungen am System Kupfer Schwefel bei Temperaturen T = 15–90 °C. *Z. Phys. Chem.* **1972**, *79*, 315–330. [[CrossRef](#)]
44. Pósfai, M.; Buseck, P. Djurleite, digenite, and chalcocite: Intergrowths and transformations. *Am. Mineral.* **1994**, *79*, 308–315.
45. Zhou, X.; Soldat, A.C.; Lind, C. Phase selective synthesis of copper sulfides by nonhydrolytic sol-gel methods. *RSC Adv.* **2014**, *4*, 717–721. [[CrossRef](#)]
46. Large, D.; MacQuaker, J.; Vaughan, D.; Sawłowicz, Z.; Gize, A.P. Evidence for Low-Temperature Alteration of Sulfides in the Kupferschiefer Copper Deposits of Southwestern Poland. *Econ. Geol.* **1995**, *90*, 2143–2155. [[CrossRef](#)]